

# Altered Modularity and Disproportional Integration in Functional Networks are Markers of Abnormal Brain Organization in Schizophrenia

Cinelli, M.<sup>1,+</sup>, Echegoyen, I.<sup>2,3,+</sup>, Oliveira, M.<sup>4,+</sup>, Orellana, S.<sup>5,+</sup>, and Gili, T.<sup>6,\*</sup>

<sup>1</sup>University of Rome "Tor Vergata", Rome, Italy

<sup>2</sup>Centre for Biomedical Technology, Technical University of Madrid, Madrid, Spain

<sup>3</sup>Rey Juan Carlos University, Madrid, Spain

<sup>4</sup>GESIS – Leibniz Institute for the Social Sciences, Cologne, Germany

<sup>5</sup>Utrecht University, Utrecht, Netherlands

<sup>6</sup>IMT School for Advanced Studies, Lucca, Italy

\*tommaso.gili@imtlucca.it

+These authors contributed equally to this work.

## ABSTRACT

Modularity plays an important role in brain networks' architecture and influences its dynamics and the ability to integrate and segregate different modules of cerebral regions. Alterations in community structure are associated with several clinical disorders, specially schizophrenia, although its time evolution is not clear yet. In the present work, we analyze fMRI functional networks of 65 healthy subjects (HC) and 44 patients of schizophrenia (SZ), 28 of them in a chronic state (CR) of illness, and 16 at early stage (ES). We find clear differences in edges' weights distribution, networks density, community structure consistency and robustness against edge removal. In comparison to healthy subjects, we found that networks from SZ patients exhibits wider weight distribution, larger overall connectivity, and are more consistent in the community structure across subjects. We also showed that the networks of SZ patients tend to be more robust to edge removal than healthy subjects, while having lower network density. In the case of early stages patients, we found that their networks exhibit topological features consistently in between the ones obtained from the other two groups, resulting in a tendency towards the chronic group state.

## Introduction

The structure and function of the brain can be conveniently characterized as a network of interacting neurons, cortical columns, or brain regions, depending on the spatial scale considered<sup>1</sup>. Both structural and functional brain networks exhibit emerging features commonly encountered in other networked systems, such as small-world structures, hubs, high assortativity, that leads to a rich-club of highly connected hubs, or modules<sup>2-4</sup>. These properties are important to ensure an efficient adaptation to the environment, and changes on them are associated with diverse pathologies<sup>5-7</sup>.

Schizophrenia is a severe psychiatric disorder that manifests through positive and negative symptoms. Positive symptoms are, among others, hallucinations, disorganized speech and delusions; whereas negative symptoms are grossly disorganized or catatonic behavior, diminished emotional expression and anhedonia. The disease is commonly accompanied with alterations in sleep, inappropriate affect, depersonalization or derealization<sup>8</sup>, and can have an insidious or sudden onset.

In classical neuroscience, researchers have developed different theories to explain the processes behind SZ, from changes in neurotransmitters, mainly dopamine, glutamate, serotonin, and  $\gamma$ -aminobutyric acid (GABA)<sup>9</sup>, to the conception of the disease as a breakdown in the integration of brain's functionally specialized processes<sup>10,11</sup>. Neuroimaging studies support these theories. Regarding functional integration, the network architecture in SZ patients tend to be more disconnected than in healthy populations<sup>12,13</sup>.

More concretely, modularity and network partitioning has proven to play an important role in shaping different topologies

between subjects suffering from SZ and healthy population<sup>14,15</sup>. A module refers to a set of nodes (i.e., brain regions) exhibiting higher connectivity among themselves in comparison to nodes outside the set<sup>16</sup>. Modules in the brain have been shown to be related to integration of information<sup>17</sup>. Healthy brains are consistently found to be within a dynamic balance between hierarchical integration and segregation of information which depends, among others, on task requirements and level of arousal<sup>18,19</sup>. This implies that information must flow to specific areas, depending on the task, and should be confined inside to be integrated for further functions, not spreading along the whole cortex. Disturbances of such balance are associated with several clinical disorders<sup>20</sup>. This relationship occurs in structural and in functional brain networks<sup>21,22</sup>, though the link between structure and function is far of being unveiled. In terms of modularity, structure and function are highly consistent, as analyses of fMRI networks tend to agree systematically<sup>23–25</sup>.

Still, different types of patients exhibit distinct features in their brain networks. In childhood onset schizophrenia, intra-module connections are lower and extra-module connections are higher than what is expected in healthy population<sup>26</sup>. In this case, modules tend to be less clearly bounded and the structural pattern tend to dissolve, preventing proper integration of information. The literature, however, diverges on adult onset schizophrenia, with results signaling both altered and intact overall modularity<sup>27,28</sup>. Yet, findings on community structure (i.e., communities in which different nodes participate) are consistent regardless of diagnostic status<sup>27–29</sup>. In these studies, however, a small but not negligible percentage of nodes is systematically placed different in schizophrenia, indicating regular changes in topology. Therefore, it is still unclear how modularity diverges in these clinical populations.

In such a complicated framework our aim is to unveil the differences concerning the community structure and the overall robustness in terms of interconnectivity of brain areas of functional networks (i.e. fMRI based) associated to healthy subjects and patients of schizophrenia. The first goal is accomplished by comparing different community structures across classes of patients in order to find cross similarities/differences. The second goal is accomplished by looking at the size of the largest connected component after the removal of links among the different brain areas using a thresholding logic which penalizes those with the lowest weights. Our findings provide insights about actual topological differences among healthy and unhealthy subjects in terms of homogeneity of partitions and fragility of the network with not negligible differences also between two classes of SZ patients (i.e. early stage and chronic schizophrenia). Nevertheless, the obtained results constitute also a base for discerning the quality of different methods concerning the study of fMRI (and in general dense) networks.

## Methods

### Subjects and clinical assessment

We recruited forty four patients diagnosed with schizophrenia according to the DSM-IV- TR (APA, 2000) criteria (SZ group). All patients were diagnosed by one senior clinical psychiatrist using the structured clinical interview for DSM-IV- TR (SCID-IP)<sup>30</sup>. Other inclusion criteria were: 1) age between 18 and 65 years; 2) at least 8 years of education; 3) no dementia or cognitive deterioration according to the DSM-IV- TR criteria, and a Mini- Mental State Examination (MMSE)<sup>31</sup> score higher than 24, consistent with normative data in the Italian population<sup>32</sup>; and 4) suitability for a Magnetic Resonance Imaging (MRI) scan. Exclusion criteria were: 1) a history of alcohol or drug dependence or abuse in the last two years according to the DSM-IV- TR, 2) traumatic head injury, 3) any past or present major medical or neurological illness, 4) any other psychiatric disorder or mental retardation diagnosis and 5) MRI evidence of focal parenchymal abnormalities or cerebrovascular diseases.

All patients were in a phase of stable clinical compensation. Age at onset was defined as age at first hospitalization or, when possible, age at onset of positive or negative symptoms prior to the first hospitalization. Out of the initial sample of 44 patients, 16 were considered being at early stages of symptoms (the period from the first psychotic symptoms and the diagnosis was shorter than two years), while 28 were considered chronic patients (the history of illness from the diagnosis of illness was longer than five years).

The Positive and Negative Syndrome Scale (PANSS)<sup>33</sup> was administered to rate severity of psychopathological symptoms. PANSS ratings were obtained on all information available pertaining to the last week of the assessment. Extrapyramidal side effects due to current treatment were assessed by the Simpson-Angus Rating Scale (SARS)<sup>34</sup>. The Abnormal Involuntary Movements Scale<sup>35</sup> was administered to determine whether tardive dyskinesia was present; however, no patient suffered from this disturbance. All patients were receiving stable oral doses of one or more atypical antipsychotic drugs such as risperidone, quetiapine, or olanzapine. Antipsychotic dosages were converted to estimated equivalent dosages of olanzapine by using a standard table<sup>36</sup>.

We also recruited 65 healthy controls in the same geographical area, so that all the subjects recruited for the study were homogeneous with regard to ethnicity and cultural background. They were rigorously matched for age, education and gender with the patients diagnosed as having schizophrenia. All HC were screened for any current or past diagnosis of DSM-IV- TR axis I or II disorders using the SCID-I and SCID-II<sup>30</sup>. A diagnosis of schizophrenia or any other mental disorder in first-degree relatives was also an exclusion criterion.

Our local Ethics Committee approved the study protocol. Written informed consent was obtained from all patients after they received a full explanation of the study procedures.

## Data acquisition and processing

MRI data were collected using gradient-echo echo-planar imaging at 3T (Philips Achieva) using a (T2\*)-weighted imaging sequence sensitive to blood oxygen level-dependent (BOLD) signal (TR = 3s, TE = 30ms, matrix = 80x80, FOV = 224x224, slice thickness = 3mm, flip angle = 90°, 50 slices). A thirty-two channel receive-only head coil was used. A high-resolution T1 weighted whole-brain structural scan was also acquired (1x1x1mm voxels). Subjects were asked to lay at rest in the scanner with eyes open. For the purposes of accounting for physiological variance in the time-series data, cardiac and respiratory cycles were recorded using the scanner's built-in photoplethysmograph and a pneumatic chest belt, respectively.

The human brain was segmented into 278 macro-regions from the template proposed by Shen et al.(2013)<sup>37</sup>. Resting state fMRI signals were averaged across each region to generate 278 time-series. Several sources of physiological variance were removed from each individual subject's time series fMRI data. For each subject, physiological noise correction consisted of removal of time-locked cardiac and respiratory artifacts (two cardiac harmonics and two respiratory harmonics plus four interaction terms), using linear regression<sup>38</sup>, and of low-frequency respiratory and heart rate effects<sup>39-41</sup>.

fMRI data were then preprocessed as follows: correction for head motion and slice-timing and removal of non-brain voxels<sup>1</sup>. Using custom software written in Matlab (The Math Work); data were demeaned and detrended, the six parameters obtained by motion realignment and their derivatives were regressed out. Further nuisance regressors were removed as sources of unwanted signals coming from white matter (WM) and cerebral spine fluid (CSF). Specifically, we calculated the first six principal components of the BOLD signal in two eroded masks that included both the ventricles and the white matter region, respectively<sup>42</sup>. Head motion estimation parameters were used to derive the frame-wise displacement (FD) and the root mean square value of the differentiated BOLD time series (DVARS): time points with high FD and DVARS (FD > 0.2 mm and DV > 20) were replaced through a least-squares spectral decomposition as described in Power et al. (2014)<sup>43</sup>. Data were then band-pass filtered in the frequency range 0.01 – 0.1 Hz, using a zero-phase second order Butterworth filter.

Since the template proposed by Shen et al.<sup>37</sup> was in the MNI standard space, a two-step registration process was performed. FMRI data were transformed, first, from functional space to individual subjects' structural space using FLIRT (FMRIB's Linear Registration Tool) and then non-linearly to a standard space (Montreal Neurological Institute MNI152 standard map) using Advanced Normalization Tools<sup>2</sup>. Finally data were spatially smoothed (5x5x5 mm full-width half-maximum Gaussian kernel).

## Functional Networks

From each subject we estimate connectivity among regions of interest (ROIs, as extracted from the atlas) pair-wise with Pearson correlation coefficient ( $r$ ). It is known that  $r$  is not always the best option, as brain time series are considered non-stationary and non-linearly coupled<sup>44</sup>. However, at small time scales, stationary and linear approximations to coupling are good enough<sup>45</sup>. This is precisely the case with the analyzed dataset. Each of the 278 areas considered comprises a time series of 180 samples at a resolution of 3 Hz. For and each subject, we obtain a functional network in which nodes are ROIs and edges are the normalized value of  $r$ . Normalization is calculated by permutation test, a common procedure of surrogate analysis, extensively used in neuroscience since the seminal work of Schreiber and Schmitz<sup>46</sup>, and proven to offer a good estimation of the real correlation between time series<sup>47-49</sup>. The method is as follows: randomize the original time series, compute  $r$  and repeat the whole process. 1000 iterations allow a robust recovery of the distribution of values under the null hypothesis of no relationship between nodes, and approaches a Gaussian distribution as the number of iterations increases. Then, the actual value obtained without randomization ( $r_{ij}$ ) is linearly normalized as a common  $z$ -score, that is,  $\hat{r}_{ij} = \frac{r_{ij} - \mu_0}{\sigma_0}$ , where  $\mu_0$  is the mean of the null distribution, and  $\sigma_0$  its deviation; and its probability is calculated. Randomization implies destroying temporal coupling among

<sup>1</sup>Removal performed using FSL: FMRIB's Software Library, [www.fmrib.ox.ac.uk/fsl](http://www.fmrib.ox.ac.uk/fsl)

<sup>2</sup>ANTS; Penn Image Computing & Science Lab, <http://www.picsl.upenn.edu/ANTS/>

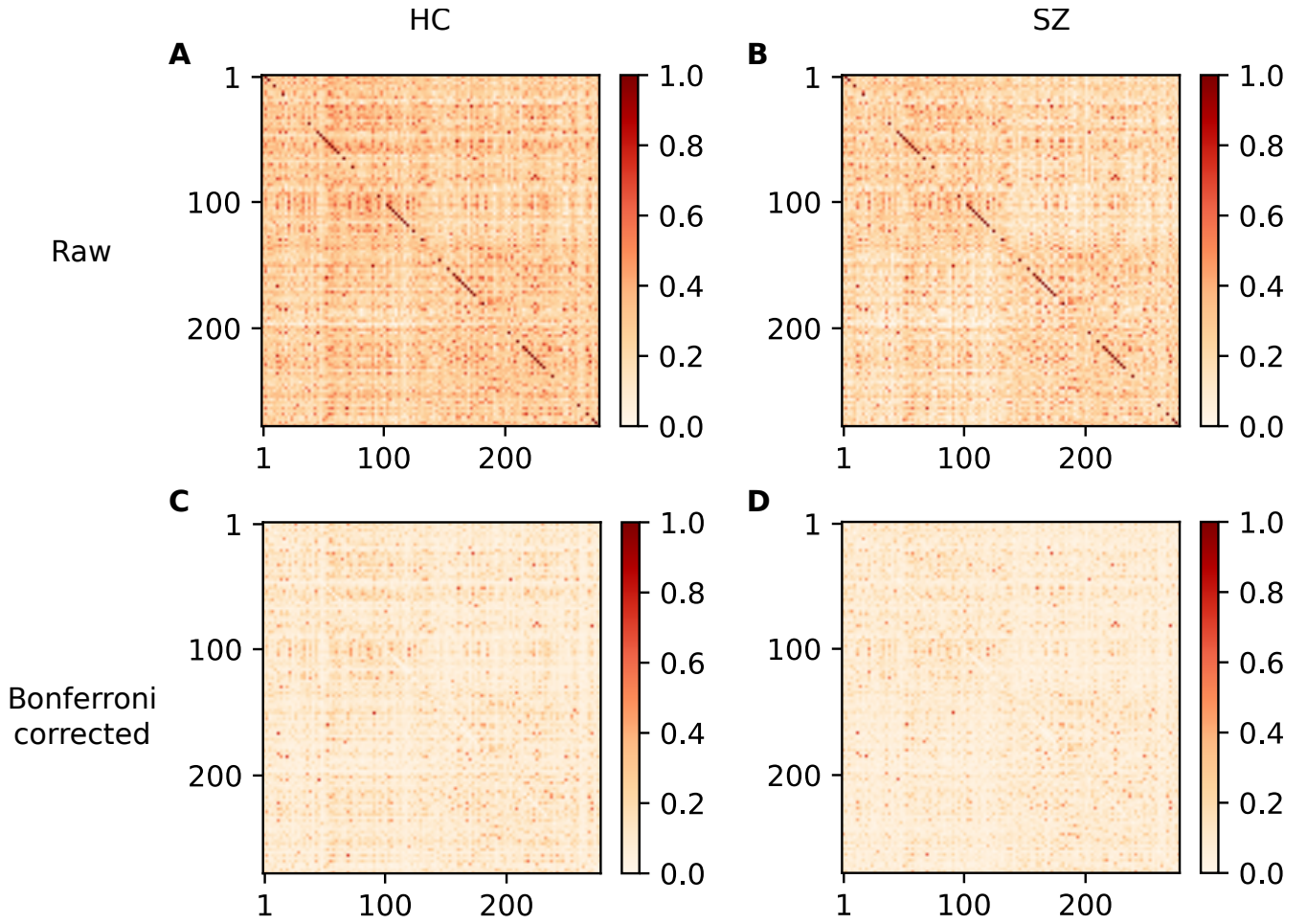


**Figure 1. Average connectivity for HC and SZ.** Upper row matrices correspond to non corrected connectivity. Bottom row matrices contain connectivity after Bonferroni correction. Leftmost matrices correspond to the average connectivity of healthy patients (HC), and rightmost matrices correspond to schizophrenia patients (SZ)

ROIs while maintaining the distribution of values. Thus, the null distribution obtained randomizing defines the probability of finding a concrete value of the edge by chance, in the case of no temporal correlation. This procedure allows us to set a threshold at  $p = 0.01$  and keep only those edges more unlikely than this probability. As the number of comparisons increases with the number of nodes ( $N \times (N - 1)$ ), we correct the  $p$ -value with the Bonferroni correction procedure. Although it is the most conservative method, it is also true that the networks become notably sparser, making community detection much more effective, as only significant edges will be conserved (thus revealing the fundamental structure of the modules). The amount of information loss in comparison with the gain in the ability to detect the communities makes it the best method to correct the  $p$  value. The corrected  $p$  value is  $3.25 \times 10^{-7}$ ). Every edge whose probability is above this threshold is set to zero, and the whole matrix is squared, making positive all edges. Fig. 1 shows the result of this procedure for groups averaged connectivity.

### Community Detection and Partitions Comparison

The process of discovery of naturally emerging groups from the network topology is commonly referred to as community detection. An established way of splitting the network into communities is represented by the modularity ( $Q$ ) maximization<sup>50</sup>. Modularity is a quantity that represents the correlation among the node attributes (i.e. assignment to communities) computed across network edges; it can be considered as a proxy for the quality of partitions. Therefore, modularity represents a quantity that needs to be optimized when performing community detection and it can be written as:

$$Q = \sum_{i,j} (A_{i,j} - \frac{k_i k_j}{2m}) \delta(c_i, c_j) \quad (1)$$

where  $A_{i,j}$  is the adjacency matrix (or weights matrix) of the network,  $k_i$  is the degree (strength) of the node  $i$ ,  $c_i$  represents the community to which vertex  $i$  is assigned,  $\delta$  is the Kronecker delta function and  $m$  is the number of network links.

Among the various algorithms for modularity maximization, we adopt an heuristic method called the Louvain method<sup>51</sup>. Usually, it provides high results in terms of modularity, thus high quality of the discovered community structure and fast computation times. The Louvain approach, however, may present suffers from the resolution limit, similarly to all the other methods which employ modularity maximization<sup>52</sup>. The resolution limit determines the performance in the identification of relatively small communities, and may yield poor results in some cases. Thus, in our study, we also detect communities using the so-called Surprise algorithm<sup>53</sup>, enabling us to evaluate how the resolution limit problem affects the quality of the retrieved community structure.

Surprise algorithm works by maximizing a quantity called Surprise that represents the probability to find edges between nodes in the same partition (i.e., community). This measure can be defined using an information-theoretic perspective with the Kullback-Leibler divergence, allowing a fast computation<sup>54</sup>. The algorithm maximizes this measure by modifying the partition assignment in the network and aggregating the communities. This procedure overcomes the resolution limit issue<sup>54</sup> and gives us meaningful partitions of the processed topologies.

In order to compare the various partitions in communities (one per subject) we use the rand index<sup>55</sup>. This measure gives us the similarity among clusters based on the frequency of elements sharing the same/different allocation. We exploit the rand index instead of its adjusted version since we are comparing partitions obtained with the same method across different networks (and not different methods of community detection on the same network).

## Results

Density in networks changed from around 0.735 (normalizing by the number of nodes) to around 0.52 after applying Bonferroni correction. This can be qualitatively observed from the heatmaps displayed in Fig. 1.

As shown in Fig. 2, the distribution of weights is different between groups. Confirming this qualitative observation, a KS test of distribution differences yield a  $p$  value of 0.0001, indicating to reject the null hypothesis of equal distributions. The same result in hypothesis testing was obtained with a previous shuffling of 200 iterations ( $p$  value = 0.001) Average level of synchronization is higher, and the distribution is wider. In the HC, values of synchronization are lower, but more concentrated.

Interestingly, differences are clearer when we take into account the two different SZ groups (early stage and chronic state). This is due to the fact that the early stage group has a more bimodal distribution, with clear tendency toward both groups (HC and SZ chronic). As the early stage group is composed of patients that has been suffering the disease and receiving treatment

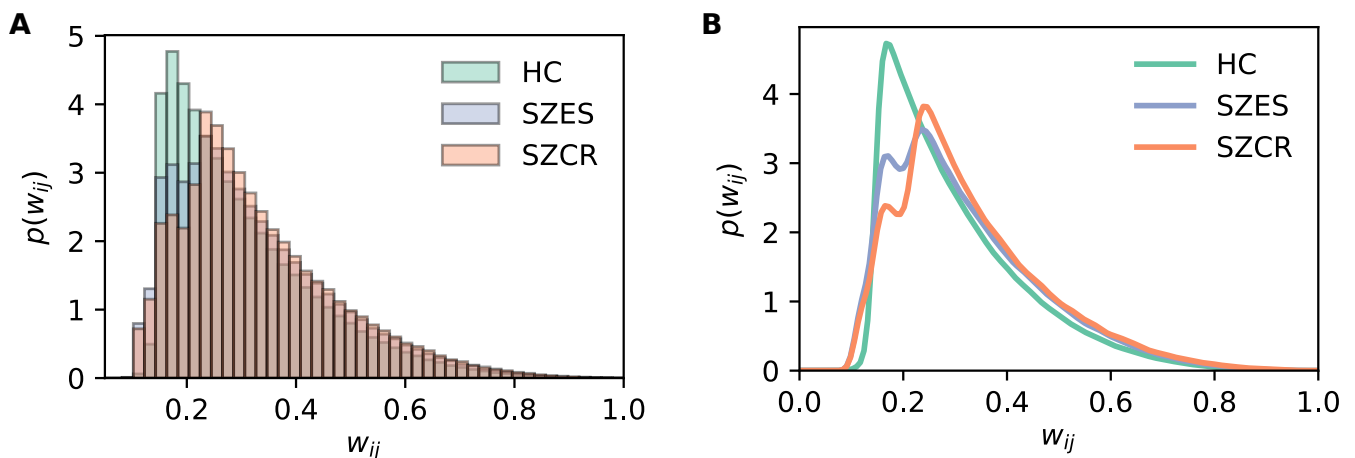


**Figure 2. Distribution of weights for the HC and SZ (ES and CR) groups.** There are significant differences between all groups' distributions ( $p < 0.001$ ). SZ (CR) patients exhibit a wider distribution, with higher overall connectivity. ES patients are in between the other two groups.

for a shorter period of time, it is reasonable to interpret that as time goes by, the disease stabilizes at a different distribution of weights (a different patterns of synchronization). Hence, what we are observing in the early SZ group is the transition to that point. This increase in synchronization could be interpreted as a compensatory mechanism for the alterations in communities, as other studies have reported<sup>14</sup>. It also may be an indirect effect of medication, as neurotransmitters play a major role in populations' coupling.

Fig. 3 shows the output of the comparison between the different partitions into communities by means of two algorithms, namely Louvain and Surprise. We firstly note how the Louvain method (Fig. 4A and Fig. 4C) suffers from the resolution limit being able to report fewer communities with a higher number of nodes as shown in Fig. 3. Conversely, partitions obtained with the Surprise method are characterized by a lower number of nodes and are thus able to capture more precisely the inner modular structure of the considered functional networks. The comparison among partitions obtained with the Surprise method suggest a higher similarity among the topologies related to schizophrenic patients shedding light on the relative similarity across such functional networks.

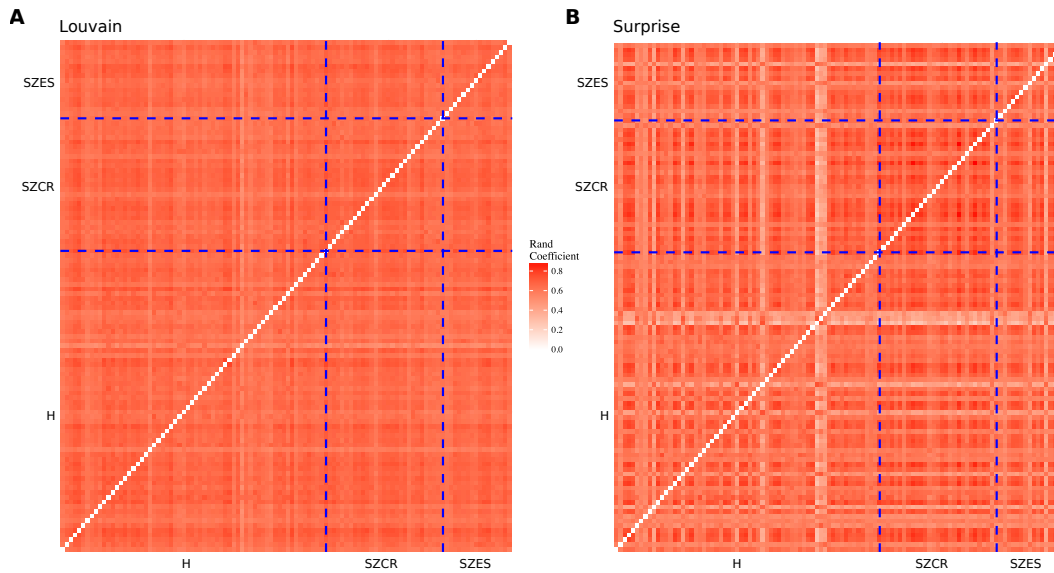


**Figure 3. The rand coefficient related to the community structure for different subjects.** The Louvain algorithm (A) is unable to detect difference between classes of patients, while the Surprise algorithm (B) identifies homogeneity between individuals of the same class.

Both community detection methods yield similar results, although the surprise algorithm allow a better understanding on the consistency of communities. SZ patients have more consistent communities, meaning that communities tend to recruit the same nodes, while the HC group shows a higher heterogeneity. This could mean that SZ patients have a more rigid configuration of communities, losing flexibility; and vice versa, the HC group shows a more flexible configuration. This is indicated by the rand index, a validated method to compare communities among groups.

Fig. 5 depicts the effect of raising the threshold of functional connectivity. As the threshold increases, density and size of the giant component decreases. Given that average synchronization is higher in the SZ group, the giant component is more robust than in the HC group. Surprisingly, density is notably smaller in the chronic group in comparison to the other two groups. HC group is more dense, and early stage SZ group is in-between, indicating that, due to the disease or to its medication, density tends to decrease with years, making the giant component more robust. That is, even though functional networks are less dense in SZ patients, they are also more robust to disconnection of the giant component, and this tendency increases with time. As far as we know, this is a novel finding not reported before in the literature.

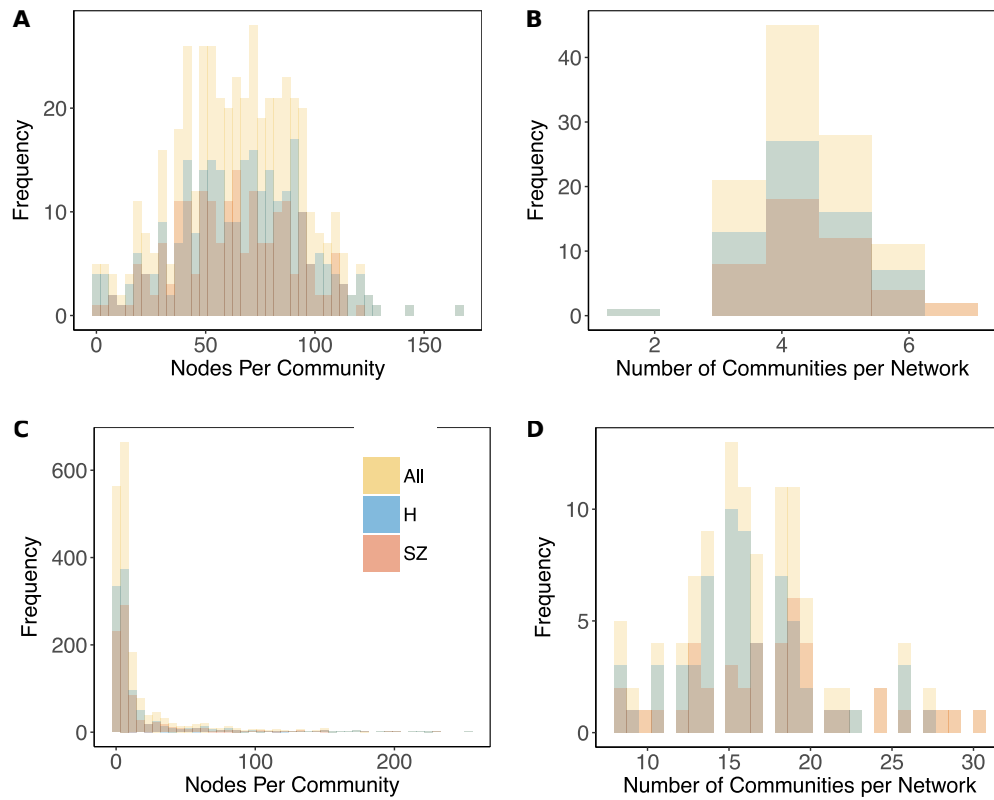


**Figure 4. Composition of communities found in the networks.** The Louvain algorithm (**A** and **B**) tends to find smaller communities than the Surprise algorithm (**C** and **D**).

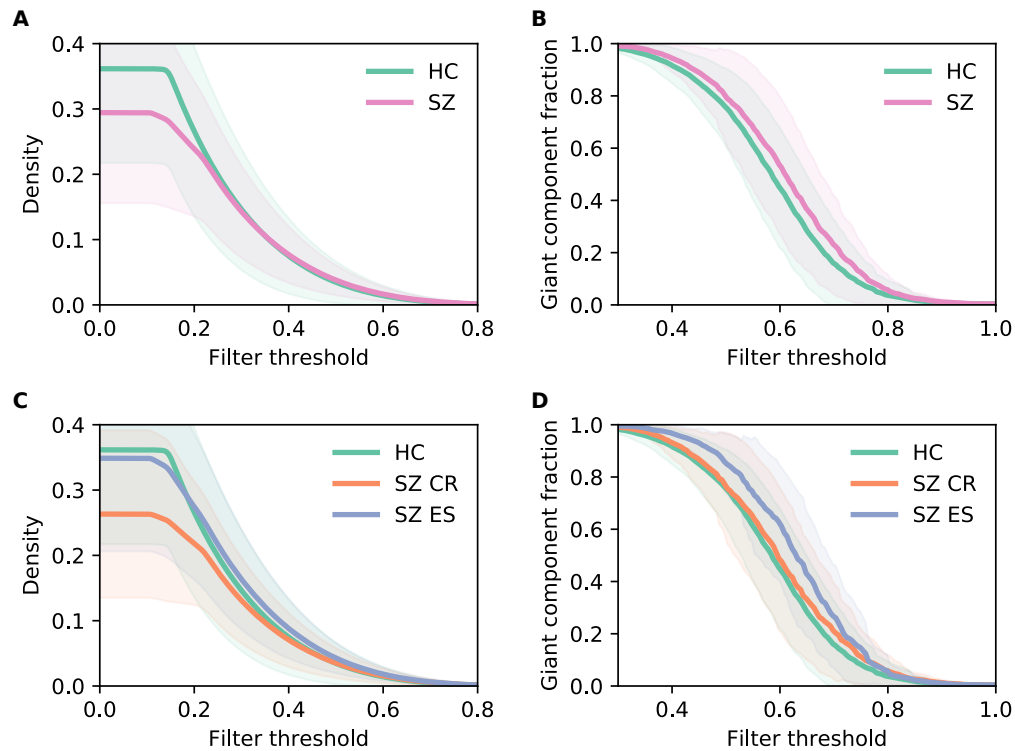


**Figure 5. Effect of the threshold on density and giant component.** Upper row show values for HC and SZ, and bottom row distinguishes also SZ subgroups (CR and ES). Leftmost plots display changes in edge density as a function of the threshold, while rightmost plots do for the size of the giant component

## Discussion and Stylized Facts

In the present paper we have shown major differences in weight distributions between SZ (ES and CR) and HC, and reported a novel finding: while SZ patients functional networks' are less dense than healthy ones, the giant component tend to be more robust to edge removal. Also, communities tend to be more consistent among those suffering from schizophrenia, possibly indicating a lack of flexibility in functional community configuration. It is possible that heterogeneous methodological choices influence the discrepancies in modularity findings, specially given the difficulties to assess the quality of the partitions produced by any algorithm (regarding inconsistent results in reported modularity between early onset).

As stated before, the analysis of the Rand Index computed over the partitions obtained with the Surprise algorithm reveals that healthy patients display a larger variability in terms of their community structure which can be considered more reconfigurable. At the same time, schizophrenia patients display a more homogeneous distribution of partitions among the network nodes implying a less reconfigurable and thus more rigid functional topology. This is in accordance with existing literature<sup>15</sup>.

The probability functions related to edge weights (i.e. correlation in activity between pairs of ROIs) differ between groups, with each one having a distinct peak. In particular, the peaks of the distribution had a higher value in chronic schizophrenia patients, compared to controls and those who had received a recent diagnosis. This could imply that connectivity between pairs of regions has the tendency progress with disease.

fMRI literature on schizophrenia often reports a lower overall connectivity in schizophrenia<sup>56</sup>. This is likely given by the higher sparsity of patient derived networks. However, as highlighted above, the existing connections tend to display a stronger weight profile. Notably, in spite of the higher sparsity, patients display a higher robustness to link removal by means of edge weight thresholding. This aspect may be related to the networks structure of the healthy subjects which may display a relatively connected core together with a more uniform distribution of edge weights.

## Future Work

As a follow up to the present paper the following steps are proposed:

- Pursuing a resilience analysis based on static/dynamic failures of nodes/edges.
- Computing the differences in efficiency of communication among brain areas by means of global/local efficiency measure.
- Considering spatial location and anatomical characterization of the network nodes and of the subjects characteristics (i.e. add to the analysis further variables represented by the meta-data of both the nodes and the network).
- The present study allows for a proper characterization of the synchronization distribution of both populations (HC and SZ). A follow step would be the extraction of both distributions, in order to allow for further simulations of resting state dynamics.
- Examining whether the results found here are time dependent. Studying MEG/EEG could allow to answer this question, and these results should be recovered in slow frequency bands.

## Acknowledgements

This work is the output of the Complexity72h workshop, held at IMT School in Lucca, 7-11 May 2018. <https://complexity72h.weebly.com/>

## References

1. Sporns, O. *Networks of the brain* (MIT Press, Cambridge, Massachusetts, 2011).

2. Bullmore, E. & Sporns, O. Complex brain networks: graph theoretical analysis of structural and functional systems. *Nat. Publ. Group* **10**, 186–198 (2009). DOI 10.1038/nrn2575.
3. Bassett, D. S. & Sporns, O. Network neuroscience. *Nat. Neurosci.* **20** (2017). DOI 10.1038/nn.4502.
4. Papo, D. *et al.* Las redes funcionales bajo la perspectiva de la teoría de grafos. In Maestú, F., del Pozo, F. & Pereda, E. (eds.) *Conectividad Funcional y Anatómica en el Cerebro Humano*, 81–91 (2015). DOI 10.1016/B978-84-9022-525-7.00008-0.
5. Bassett, D. S. & Bullmore, E. T. Human brain networks in health and disease. *Curr. opinion neurology* **22**, 340–7 (2009). DOI 10.1097/WCO.0b013e32832d93dd.
6. Griffa, A., Baumann, P. S., Thiran, J.-P. & Hagmann, P. Structural connectomics in brain diseases. *NeuroImage* **80**, 515–26 (2013). DOI 10.1016/j.neuroimage.2013.04.056.
7. Kaiser, M. The potential of the human connectome as a biomarker of brain disease. *Front. human neuroscience* **7**, 484 (2013). DOI 10.3389/fnhum.2013.00484.
8. Association, A. P. *Diagnostic and statistical manual of mental disorders* (Washington, DC, 2013), 5th edn.
9. Schulz, S. C., Green, M. F. & Nelson, K. J. *Schizophrenia and Psychotic Spectrum Disorders* (Oxford, UK).
10. Fodor, J. A. Precis of the modularity of mind. *Behav. brain sciences* **8**, 1–5 (1985).
11. David, A. S. Dysmodularity: A neurocognitive model for schizophrenia. *Schizophr. Bull.* (1994).
12. Fornito, A., Zalesky, A., Pantelis, C. & Bullmore, E. T. Schizophrenia, neuroimaging and connectomics. *Neuroimage* **62**, 2296–2314 (2012).
13. van den Heuvel, M. P. & Fornito, A. Brain networks in schizophrenia. *Neuropsychol. review* **24**, 32–48 (2014).
14. Sun, Y., Dai, Z., Li, J., Collinson, S. L. & Sim, K. Modular-level alterations of structure–function coupling in schizophrenia connectome. *Hum. brain mapping* **38**, 2008–2025 (2017).
15. Reinen, J. M. *et al.* The human cortex possesses a reconfigurable dynamic network architecture that is disrupted in psychosis. *Nat. communications* **9**, 1157 (2018).
16. Newman, M. E. & Girvan, M. Finding and evaluating community structure in networks. *Phys. review E* **69**, 026113 (2004).
17. Sporns, O. Network attributes for segregation and integration in the human brain. *Curr. Opin. Neurobiol.* **23**, 162–171 (2013). DOI 10.1016/j.conb.2012.11.015.
18. Buzsáki, G. *Rhythms of the brain* (2006). DOI 10.1093/acprof:oso/9780195301069.001.0001.
19. Sporns, O. & Betzel, R. F. Modular brain networks. *Annu. Rev. Psychol.* **67**, 613–640 (2016). DOI 10.1146/annurev-psych-122414-033634.
20. Bullmore, E. & Sporns, O. The economy of brain network organization. *Nat Rev Neurosci* **13**, 336–349 (2012). DOI 10.1038/nrn3214.
21. Meunier, D., Lambiotte, R., Fornito, A., Ersche, K. D. & Bullmore, E. T. Hierarchical modularity in human brain functional networks. *Front. Neuroinformatics* **3**, 37 (2009). DOI 10.3389/neuro.11.037.2009.
22. Tononi, G., Sporns, O. & Edelman, G. M. A measure for brain complexity: relating functional segregation and integration in the nervous system. *Proc. Natl. Acad. Sci.* **91**, 5033–5037 (1994).
23. Meunier, D., Lambiotte, R. & Bullmore, E. T. Modular and hierarchically modular organization of brain networks. *Front. neuroscience* **4**, 200 (2010).
24. Hagmann, P. *et al.* Mapping the Structural Core of Human Cerebral Cortex. *PLOS Biol.* **6**, e159 (2008). DOI 10.1371/journal.pbio.0060159.
25. Chen, Z. J., He, Y., Rosa-Neto, P., Germann, J. & Evans, A. C. Revealing modular architecture of human brain structural networks by using cortical thickness from mri. *Cereb. cortex* **18**, 2374–2381 (2008).
26. Alexander-Bloch, A. F. *et al.* Disrupted modularity and local connectivity of brain functional networks in childhood-onset schizophrenia. *Front. systems neuroscience* **4**, 147 (2010).
27. Yu, Q. *et al.* Modular organization of functional network connectivity in healthy controls and patients with schizophrenia during the resting state. *Front. systems neuroscience* **5**, 103 (2012).
28. Lerman-Sinkoff, D. B. & Barch, D. M. Network community structure alterations in adult schizophrenia: identification and localization of alterations. *NeuroImage: Clin.* **10**, 96–106 (2016).

29. Alexander-Bloch, A. *et al.* The discovery of population differences in network community structure: new methods and applications to brain functional networks in schizophrenia. *Neuroimage* **59**, 3889–3900 (2012).
30. MB., F., RL., G. M. S., JBW., W. & LS., B. *Interview for DSM-IV Axis II Personality Disorders, (SCID-II)* (American Psychiatric Press, Inc., Washington, D.C., 1997).
31. Folstein, M. F., Folstein, S. E. & McHugh, P. R. “mini-mental state”: A practical method for grading the cognitive state of patients for the clinician. *J. Psychiatr. Res.* **12**, 189 – 198 (1975). DOI [https://doi.org/10.1016/0022-3956\(75\)90026-6](https://doi.org/10.1016/0022-3956(75)90026-6).
32. Measso, G. *et al.* The mini-mental state examination: Normative study of an italian random sample. *Dev. Neuropsychol.* **9**, 77–85 (1993). DOI [10.1080/87565649109540545](https://doi.org/10.1080/87565649109540545).
33. SR., K., A., F. & LA., O. *Schizophr. Bull.* **13** (1987).
34. M., S. G. *et al.* A rating scale for extrapyramidal side effects. *Acta Psychiatr. Scand.* **45**, 11–19 (1970). DOI [10.1111/j.1600-0447.1970.tb02066.x](https://doi.org/10.1111/j.1600-0447.1970.tb02066.x).
35. W., G. Abnormal involuntary movement scale (aims). In W., G. (ed.) *ECDEU assessment manual for psychopharmacology*, 534–537 (Department of Health Education and Welfare, Washington, D.C., 1976).
36. Chlorpromazine equivalent doses for the newer atypical antipsychotics. *J. Clin. Psychiatry* (2003).
37. Shen, X., Tokoglu, F., Papademetris, X. & Constable, R. T. Groupwise whole-brain parcellation from resting-state fMRI data for network node identification. *NeuroImage* **82**, 403–415 (2013). DOI [10.1016/j.neuroimage.2013.05.081](https://doi.org/10.1016/j.neuroimage.2013.05.081).
38. H., G. G., Tie-Qiang, L. & David, R. Image-based method for retrospective correction of physiological motion effects in fmri: Retroicor. *Magn. Reson. Medicine* **44**, 162–167 (2000). DOI [10.1002/1522-2594\(200007\)44:1;162::AID-MRM23;3.0.CO;2-E](https://doi.org/10.1002/1522-2594(200007)44:1;162::AID-MRM23;3.0.CO;2-E).
39. M., B. R., B., D. J., A., S. M. & A, B. P. Separating respiratory-variation-related fluctuations from neuronal-activity-related fluctuations in fmri. *NeuroImage* **31**, 1536 – 1548 (2006). DOI <https://doi.org/10.1016/j.neuroimage.2006.02.048>.
40. Chang, C. & Glover, G. H. Effects of model-based physiological noise correction on default mode network anti-correlations and correlations. *NeuroImage* **47**, 1448 – 1459 (2009). DOI <https://doi.org/10.1016/j.neuroimage.2009.05.012>.
41. Shmueli, K. *et al.* Low-frequency fluctuations in the cardiac rate as a source of variance in the resting-state fmri bold signal. *NeuroImage* **38**, 306 – 320 (2007). DOI <https://doi.org/10.1016/j.neuroimage.2007.07.037>.
42. Behzadi, Y., Restom, K., Liau, J. & Liu, T. T. NIH Public Access. *NeuroImage* **37**, 1301–1315 (2007). DOI [10.1007/s10439-011-0452-9](https://doi.org/10.1007/s10439-011-0452-9).Engineering.
43. Power, J. D. *et al.* Methods to detect, characterize, and remove motion artifact in resting state fmri. *NeuroImage* **84**, 320 – 341 (2014). DOI <https://doi.org/10.1016/j.neuroimage.2013.08.048>.
44. Stam, C. J. Nonlinear dynamical analysis of EEG and MEG: Review of an emerging field. *Clin. Neurophysiol.* **116**, 2266–2301 (2005). DOI [10.1016/j.clinph.2005.06.011](https://doi.org/10.1016/j.clinph.2005.06.011).
45. Sakkalis, V. Review of advanced techniques for the estimation of brain connectivity measured with EEG/MEG. *Comput. Biol. Medicine* **41**, 1110–1117 (2011). DOI [10.1016/j.combiomed.2011.06.020](https://doi.org/10.1016/j.combiomed.2011.06.020).
46. Schreiber, T. & Schmitz, A. Surrogate time series. *Phys. D* **142**, 346–382 (2000). DOI [10.1016/S0167-2789\(00\)00043-9](https://doi.org/10.1016/S0167-2789(00)00043-9).
47. Cohen, M. X. *Analyzing Neural Time Series Data: Theory and Practice* (MIT Press, Cambridge, Massachusetts, 2014).
48. Maris, E. & Oostenveld, R. Nonparametric statistical testing of eeg-and meg-data. *J. neuroscience methods* **164**, 177–190 (2007).
49. Nichols, T. E. & Holmes, A. P. Nonparametric Permutation Tests For Functional Neuroimaging: A Primer with Examples. *Hum. Brain Mapp.* **15**, 1–25 (2001).
50. Newman, M. Modularity and community structure in networks. *Proc. Natl. Acad. Sci. United States Am.* **103**, 8577–8582 (2006).
51. Blondel, V. D., Guillaume, J.-L., Lambiotte, R. & Lefebvre, E. Fast unfolding of communities in large networks. *J. statistical mechanics: theory experiment* **2008**, P10008 (2008).
52. Fortunato, S. & Barthelemy, M. Resolution limit in community detection. *Proc. Natl. Acad. Sci.* **104**, 36–41 (2007).
53. Aldecoa, R. & Marín, I. Surprise maximization reveals the community structure of complex networks. *Sci. reports* **3**, 1060 (2013).
54. Traag, V. A., Aldecoa, R. & Delvenne, J.-C. Detecting communities using asymptotical surprise. *Phys. Rev. E* **92**, 022816 (2015).

55. Rand, W. M. Objective criteria for the evaluation of clustering methods. *J. Am. Stat. association* **66**, 846–850 (1971).
56. Zhou, Y. *et al.* Altered intrinsic and extrinsic connectivity in schizophrenia. *NeuroImage: Clin.* **17**, 704–716 (2018).